



Nano-Resveratrol Mitigates Dimethylhydrazine-Induced Colorectal Carcinogenesis in Male Rats: Impact on Oxidative Stress, Antioxidant Defense, and Radiation-augmented Pathways

Mai H. F. Othman¹, Eman I. Kandil¹, Sawsan M. Elsonbaty² and Nermeen M. Elbakary³

¹Biochemistry Department, Faculty of science- Ain Shams University, Cairo, Egypt.

²Radiation Microbiology Department, National Center for Radiation Research and Technology, Egyptian Atomic Energy Authority, Cairo, Egypt.

³Radiation Biology Department, National Center for Radiation Research and Technology, Egyptian Atomic Energy Authority, Cairo, Egypt.

Received: 05 July 2025

Accepted: 15 Sept. 2025

Published: 30 Sept. 2025

ABSTRACT

Background: Colorectal cancer remains a major cause of cancer-related mortality worldwide. Antilymphangiogenic strategies, coupled with modulation of oxidative stress and apoptotic pathways, offer potential therapeutic avenues. This study evaluated the anticancer activity of nano-resveratrol against dimethylhydrazine (DMH)-induced colon carcinogenesis in male albino rats. **Materials and Methods:** Male albino rats were allocated into five groups: Group 1 normal control receiving saline i.p. for 30 weeks; Group 2 DMH only (20 mg/kg b.w. s.c., weekly for 9 weeks); Group 3 DMH followed by resveratrol three times weekly for 21 weeks); Group 5 DMH + NRSV and exposure to low-dose gamma radiation (0.25 Gy) during the post-DMH period. Endpoints included oxidative stress markers [malondialdehyde (MDA)], reduced glutathione (GSH), total antioxidant capacity (TAC), and ROS; apoptosis was assessed by Annexin V flow cytometry. Histopathological examination of the colon was performed after euthanasia, with evaluation for dysplasia, adenomas, adenocarcinoma, and lymphangiogenesis markers where applicable. **Results:** DMH administration induced clear colonic carcinogenesis characterized by mucosal dysplasia progressing to adenocarcinoma in a subset of animals. Histopathology revealed architectural distortion, glandular atypia, increased mitotic figures, and focal invasive patterns in affected groups. Compared with normal controls, DMH-treated groups showed elevated MDA and ROS levels, with suppressed GSH and TAC, indicating oxidative stress. Annexin V analysis demonstrated increased apoptotic populations in response to DMH, reflecting compensatory cytotoxic responses. NRSV, both alone and in combination with radiation, moderated oxidative stress by reducing MDA and ROS and restoring GSH and TAC toward control levels. **Conclusion:** Nano-resveratrol demonstrated potent anticarcinogenic activity against DMH-induced colorectal carcinogenesis in male albino rats. The beneficial effect were mediated, at least in part, by attenuation of oxidative stress, restoration of antioxidant defenses, and modulation of apoptotic pathways. When combined with radiation, NRSV showed further improvement in histological and molecular endpoints, suggesting a potential combinatorial approach for colorectal cancer prevention or adjunct therapy.

Keywords: Low dose radiation, DMH, nano resveratrol, annexin V

1. Introduction

Colorectal cancer (CRC) remains one of the leading causes of cancer-related morbidity and mortality worldwide. Despite advances in screening and therapeutic strategies, the prognosis for advanced CRC remains poor, underscoring the need for novel preventive and therapeutic approaches that target not only tumor growth but also the tumor microenvironment (Zhou *et al.*, 2025). Lymphangiogenesis, the growth of new lymphatic vessels, has emerged as a critical process in tumor metastasis, facilitating tumor cell dissemination to regional lymph nodes and distant organs. The density

Corresponding Author: Mai H.F. Othman, Biochemistry Department, Faculty of science- Ain Shams University, Cairo, Egypt.

of lymphatic vessels within and around tumors correlates with metastatic spread and poorer clinical outcomes in CRC (Medhat *et al.*, 2017). Thus, agents that can suppress lymphangiogenesis may impede metastatic progression and improve patient prognosis (Medhat *et al.*, 2017)

Dimethylhydrazine (DMH) is a well-established chemical carcinogen used to induce colon carcinogenesis in rodent models that recapitulate key features of human CRC, including aberrant crypt foci, dysplasia, and adenocarcinoma. DMH- induced models have been instrumental in evaluating chemopreventive and therapeutic interventions, as they allow controlled examination of tumor initiation, progression, and the associated molecular alterations. In this context, DMH exposure reliably triggers oxidative stress, inflammatory responses, and genomic instability, creating a suitable platform to study agents with antioxidative and anti- inflammatory properties (ElBakary *et al.*, 2022).

Natural products and their derivatives have long been explored for anti-cancer properties, including anti-angiogenic and anti-lymphangiogenic effects (Deng *et al.*, 2024). Resveratrol (RSV), Resveratrol, a polyphenol found in various plants including grapes, berries, and peanuts, has gained attention in cancer research due to its wide range of potential anticancer effects. The mechanisms through which resveratrol impacts cancer cells are multifaceted, affecting various aspects of cancer biology. Its role in cancer can be particularly insightful when examined from the perspectives of the metabolic theory of cancer and the mutated stem cell theory, exhibits multiple bioactive properties, including anti-proliferative, pro- apoptotic, anti-inflammatory, and anti-angiogenic activities in various cancer models (Li *et al.*, 2025). Recent interest has focused on improving the delivery and efficacy of RSV through nanoparticle formulation, giving rise to nano-resveratrol (NRSV), which enhances cellular uptake, bioavailability, and therapeutic index (Liu *et al.*, 2025). Several studies have demonstrated that RSV can modulate signaling pathways involved in cell proliferation, apoptosis, and angiogenesis, including VEGF/VEGFR axis and related lymphangiogenic mediators, suggesting potential utility in preventing metastatic spread in CRC (Wu *et al.*, 2020). However, data on the anti-lymphangiogenic effect of NRSV in DMH-induced colon carcinogenesis, particularly in the context of oxidative stress and apoptotic regulation, remain limited.

Radiation therapy is a standard modality for various cancers and can influence the tumor vasculature and microenvironment. Low-dose gamma irradiation has been reported to modulate lymphangiogenic signaling and tumor perfusion, with complex effect that may either promote or inhibit tumor progression depending on dose and scheduling. In preclinical models, combining radioprotective or radiosensitizing interventions with anti-angiogenic or anti-lymphangiogenic agents has shown potential to enhance therapeutic efficacy while mitigating adverse effect (Gao *et al.*, 2023). The interaction between NRSV and radiation exposure in the context of DMH-induced colon carcinogenesis warrants systematic investigation to elucidate possible synergistic or antagonistic effect on tumor growth, lymphangiogenesis, oxidative stress, and apoptosis.

Oxidative stress and antioxidant defenses play pivotal roles in carcinogenesis and cancer progression. DMH-induced colorectal carcinogenesis is associated with enhanced lipid peroxidation, depletion of endogenous antioxidants, and increased reactive oxygen species (ROS), contributing to DNA damage and tumor progression. Biomarkers such as malondialdehyde (MDA), reduced glutathione (GSH), total antioxidant capacity (TAC), and ROS levels provide a comprehensive assessment of redox status and oxidative injury in CRC models. Modulation of oxidative stress by chemopreventive agents can influence apoptosis, DNA repair, and immune responses, thereby impacting tumor outcome (ElBakary *et al.*, 2022).

The lymphatic system's involvement in tumor biology extends beyond simple conduit functions to active participation in tumor cell dissemination. Lymphangiogenesis is driven by a network of pro-lymphangiogenic factors, including vascular endothelial growth factors (VEGF-C/D) and their receptors (VEGFR-3), and is supported by markers such as LYVE-1. Interventions that disrupt lymphangiogenic signaling have demonstrated reduced metastatic spread in preclinical CRC models (Zhang *et al.*, 2025). Given the proposed anti- lymphangiogenic potential of NRSV, it is rational to explore its capacity to attenuate lymphangiogenesis, thus potentially limiting metastatic risk in DMH-induced colon cancer.

This study aims to: (1) evaluate of NRSV in a DMH-induced rat model of colon carcinogenesis; (2) assess its effect on oxidative stress and antioxidant defenses (MDA, GSH, TAC, ROS); (3) quantify apoptosis via Annexin V flow cytometry; (4) examine histopathological changes in the colon and lymphangiogenic marker expression; and (5)

determine the impact of combining NRSV with low-dose gamma irradiation on tumor biology. We hypothesize that NRSV will suppress lymphangiogenesis, reduce oxidative stress, enhance antioxidant capacity, and modulate apoptotic pathways, resulting in diminished tumor burden and improved histopathology, with possible additive or synergistic effect when combined with radiation.

2. Materials and Methods

2.1. Ethics statement

The study was conducted in accordance with the recommendations in the Guide for the Use and Care of Laboratory Animals of the National Institute of Health (NIH no. 85:23, revised 1996) and in compliance with the regulations of Ethical Committee (REC) of the NCRRT, Atomic Energy Authority, Cairo, Egypt REC has approved this research protocol, following the 3Rs principles for animal experimentation (Replace, Reduce, and Refine) and is organized and operated according to the CIOMS and ICLAS International Guiding Principles for Biomedical Research Involving Animals 2012.

2.2. Drugs and chemicals

Dimethylhydrazine (DMH), Resveratrole, cisplatin, and urethane were obtained from Sigma Aldrich (Sigma-Aldrich, St. Louis, MD, USA).

2.3. facility and irradiation procedures

Rats were exposed to low dose gamma irradiation, starting after induction of colon cancer and NRSV treatment, at the NCRRT utilizing a Canadian Gamma- cell-40 (Cs137) biological irradiator (Canada Ltd. in Ottawa, Ontario, Canada).

The animals were placed in a plastic sample tray with a lid and supports for use in the sample cavity. According to the Protection and Dosimetry Department's requirements, the unit contains ventilation holes that align with ventilation sections through the main shield to give a means for uniform irradiation of small animals at a dosage rate of 0.403 Gy/min at the time of experiment.

2.4. Induction of colorectal cancer

1,2 dimethyl hydrazine (DMH) will be dissolved in 1mM EDTA just prior to use and the pH will be adjusted to 6.5 with 1mM sodium bicarbonate to ensure the stability of the chemical. Animals will be given a weekly subcutaneous (s.c) injection of DMH at a dose of 20 mg/kg body weight for 9 weeks

Experimental Design

A total number of 150 male albino rats will be randomly allocated into 7 groups as follows:

Group 1: Normal control rats (will receive 72 doses of intraperitoneal (i.p.) injection of isotonic saline solution over period of 30 weeks) 10 rats.

Group 2: Rats will receive DMH (20 mg/kg b.w. subcutaneously (s.c.) once a week for 9 weeks (20 rats).

Group 3: Rats will receive DMH (20 mg/kg b.w. subcutaneously (s.c.) once a week for 9 weeks then nano resveratrol (40 mg/kg body weight orally, 3 doses /week for 21 weeks) 20 rats.

Group 4: Rats will receive DMH (20 mg/kg b.w. subcutaneously (s.c.) once a week for 9 weeks then (20 rats) then whole body exposed to low dose gamma radiation (0.25 GY).

Group 5: Rats will receive DMH (20 mg/kg b.w. subcutaneously (s.c.) once a week for 9 weeks then nano resveratrol (40 mg/kg body weight orally, 3 doses /week for 21 weeks 20 rats) then whole body exposed to low dose gamma radiation (0.25 GY).

At the end of experimental period, animals will be anesthetised by intraperitoneal injection of urethane 1.2 g/ Kg b. wt and then scarified by confirming to death by euthanasia using cardiac acupuncture,; blood and colon tissue will be collected for biochemical analysis and molecular investigations. Colon sections will be prepared for histopathological study.

2.5. Assessment of Liver Function

Serum levels of alanine aminotransferase (ALT) and aspartate aminotransferase (AST) were measured employing colorimetric assays based on the method of Reitman and Frankel (1957).

Commercial diagnostic kits supplied by Biodiagnostic (Egypt; CAT# AL 1031 for ALT and CAT# AS 1061 for AST) were utilized.

In brief, serum samples were reacted with 2,4-dinitrophenylhydrazine (1 mmol/L) and incubated at 37°C for 30 minutes. The resulting colorimetric change was measured spectrophotometrically at 505 nm using a double-beam UV-Visible spectrophotometer (Thermo Electron, England).

2.6. Biochemical Assays

2.6.1. Assessment of Oxidative Status:

Serum malondialdehyde (MDA) levels, a marker of lipid peroxidation, were measured using the thiobarbituric acid reactive substances (TBARS) assay at 532 nm, following the protocol of Yoshioka *et al.* (1979).

2.6.2. Total Protein Content:

Total protein concentration in tissue homogenates was determined using the method described by Lowry *et al.* (1951).

2.6.3 Quantification of Total Antioxidant Capacity (TAC) and ROS

Colon tissue levels of TAC and ROS were quantified using commercially available rat-specific enzyme-linked immunosorbent assay (ELISA) kits (MyBioSource, San Diego, USA; CAT# MBS1600693 for). All assays were performed in accordance with the manufacturers' protocols.

2.6.4. Annexin V detection of apoptosis by Flow cytometry analysis

For flow cytometry, colonic tissues were dissected and minced to small clumps, followed by enzymatic dissociation with 0.5 mg collagenase IV (Sigma) in PBS for 25 min at 37°C on a shaker, and centrifuged at 500xg for 10 min. The supernatant containing debris was discarded, and the pelleted cells were washed twice with PBS and filtered through a 100 µm cell strainer to obtain a single-cell suspension. Cells were washed with cell staining buffer, centrifuged at 400 xg for 5 minutes at 4°C, and the supernatant was discarded. The pellet was then resuspended in cell staining buffer, a cell count and viability analysis were performed using trypan blue and the bright line haemocytometer where the suspension was adjusted to a concentration of 1 x 10⁶ cells/mL. Phosphatidylserine exposure on the outer leaflet of the plasma membrane was detected using the Annexin V-FITC/PI Apoptosis Detection Kit (BD pharmingen TM, BD Biosciences Co., USA; Number # 51-66121E), where cells were then resuspended in 1X Binding Buffer at a concentration of 1 x 10⁶ cells/ml. To a 5 ml culture tube, 5 µl of FITC Annexin V and 5 µl PI were added to 100 µl of the solution (1x10⁵ cells). The cells were gently vortexed and incubated for 15 min at 25°C in the dark. Finally, 400 µl of 1X Binding Buffer was added to each tube and 10,000 cells were analyzed by flow cytometry within an hour on a FACSC-LSR (Becton and Dickinson Company) equipped with Cell Quest software. Three specimens were analyzed from each group.

2.6.5. Histopathological examination

Tissue specimens were collected from colon fixed in formalin 10% and trimmed off, washed, and dehydrated in ascending concentrations of ethanol. The specimens were then cleared in xylene, embedded in paraffin blocks and sectioned at 5 µm thick. The sections were deparaffinized using xylol and stained with hematoxylin and eosin (H&E) for histopathological examination. The following morphological characteristics were assessed using the standard definitions of the World Health Organization's and the American Joint Committee on Cancer. The tumor cell architectural complexity (arbitrarily graded 1–5; 1 = simple or well differentiated, 2 = some complexity with glands containing apparent secondary structure, 3 = more complexity with glands containing tertiary structures, 4 = complex glands with some areas of solid growth, 5 = solid growth; tumor infiltrating lymphocytes, referring to lymphocytes within tumor cells and tumor nests, exclusive of stromal lymphocytes). Based on the number of lymphocytes, grade 5 has a score range of 0 to 3 (0 = none, 1 = less than 10 per medium power field, 2 = 10–20 per medium power field, 3 = more than 20 per medium power field).

2.7. Statistical analysis

The distribution of data was examined using the Kolmogorov-Smirnov test. Statistical analysis was carried out using ANOVA by GraphPad Prism® version 8.00 (San Diego, CA, USA) software followed by Tukey-HSD test for multiple comparisons. The significant differences were considered statistically at $p < 0.05$. Data were presented as mean \pm SEM.

3. Results

3.1. Macroscopic examination of colon, mortality, tumor incidence and multiplicity

There were no spontaneous tumors in the control group after 30 weeks. DMH resulted in a 70% mortality and this percentage was reduced to 60% in the monotherapy groups, and to 65% in the groups treated with Nano Resveratrole + irradiation and cisplatin + irradiation. Most of the mortalities (45-60%) occurred during the administration of DMH (9 weeks). Over the course of 21 weeks after the administration of DMH, all the treated groups lost one or two animals and had a mortality rate at 5-10% (Figure 1). DMH resulted in 100% tumor incidence. Cisplatin and irradiation equally reduced the incidence to 50%. NRSV alone reduced the incidence to 37.5%. Concomitant treatment with NRSV derivative and radiation resulted in the best reported incidence (28.5%). This last group also showed the best therapeutic effect on the tumor multiplicity. Monotherapy with NRSV derivative, radiation, or cisplatin reduced the multiplicity by ~35-46%. The combined treatment with NRSV derivative+irradiation and cisplatin+irradiation reduced the multiplicity by ~77% and 70%.

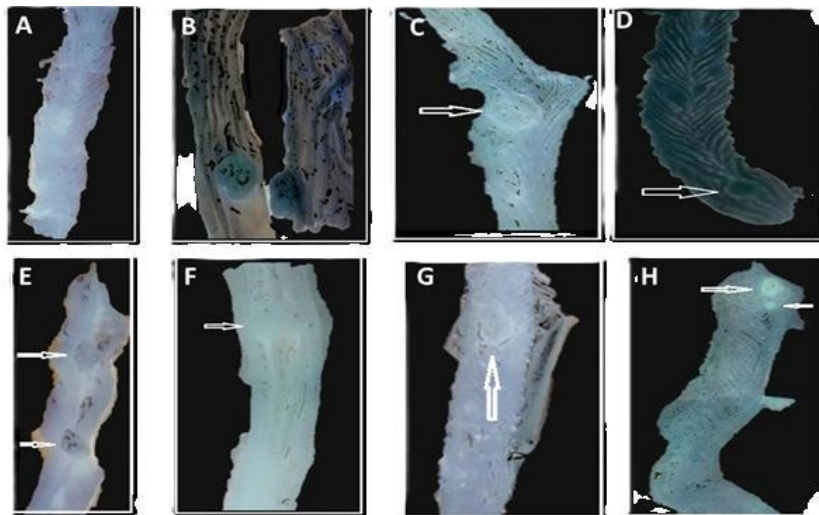


Fig. 1: Macroscopic examination of colorectal tissue from (A) Control, (B) DMH, (C) DMH +T, (F) DMH+R, (G) DMH+Cis+R, (H) DMH+T+R groups, the arrows refer to polyps of colorectal cancer

3.2. Effect of NRSV on oxidative stress

In the DMH-colon cancer model, treatment with naresveratrole significantly increased glutathione (GSH) levels compared with the DMH control, indicating a meaningful restoration of antioxidant capacity. By contrast, exposure to DMH+Cis tended to reduce GSH relative to DMH, whereas co-treatment with naresveratrole plus R or with NRSV plus R sustained elevated GSH levels, suggesting that NRSV (with or without R) promote an antioxidant response in this model. Overall, nano resveratrole appears to counteract the DMH-induced depletion of GSH and supports an enhanced antioxidant status in colon cancer tissue.

3.3. Effect of nano resveratrole on lipid peroxidation

In the DMH-colon cancer model, treatment with naresveratrole appears to influence lipid peroxidation markers, as reflected by malondialdehyde (MDA) levels. Based on the pattern observed for glutathione, NRSV-based interventions (with or without R) tend to be associated with decreased oxidative stress markers—suggesting decrease in MDA relative to the DMH control. The co- treatments involving R, particularly DMH+Cis+R or DMH+NRSV+R, show variable MDA responses, with some replicates indicating lower MDA than DMH alone

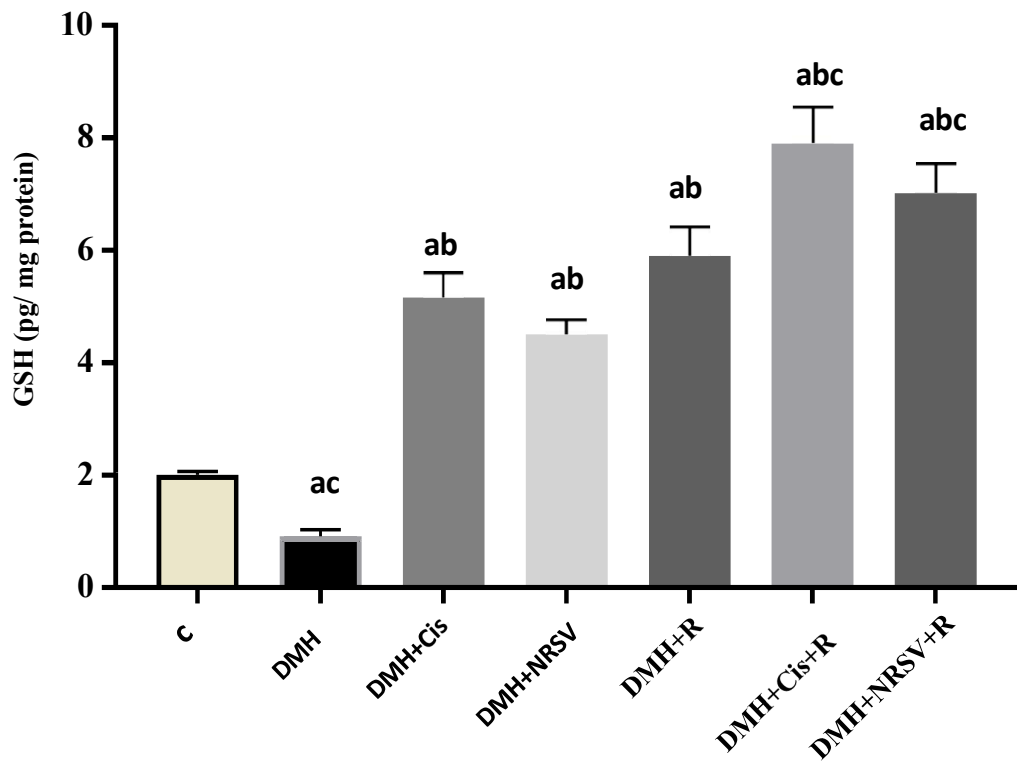


Fig. 2: Effect of resveratrole nanoparticles on glutathione level in different groups

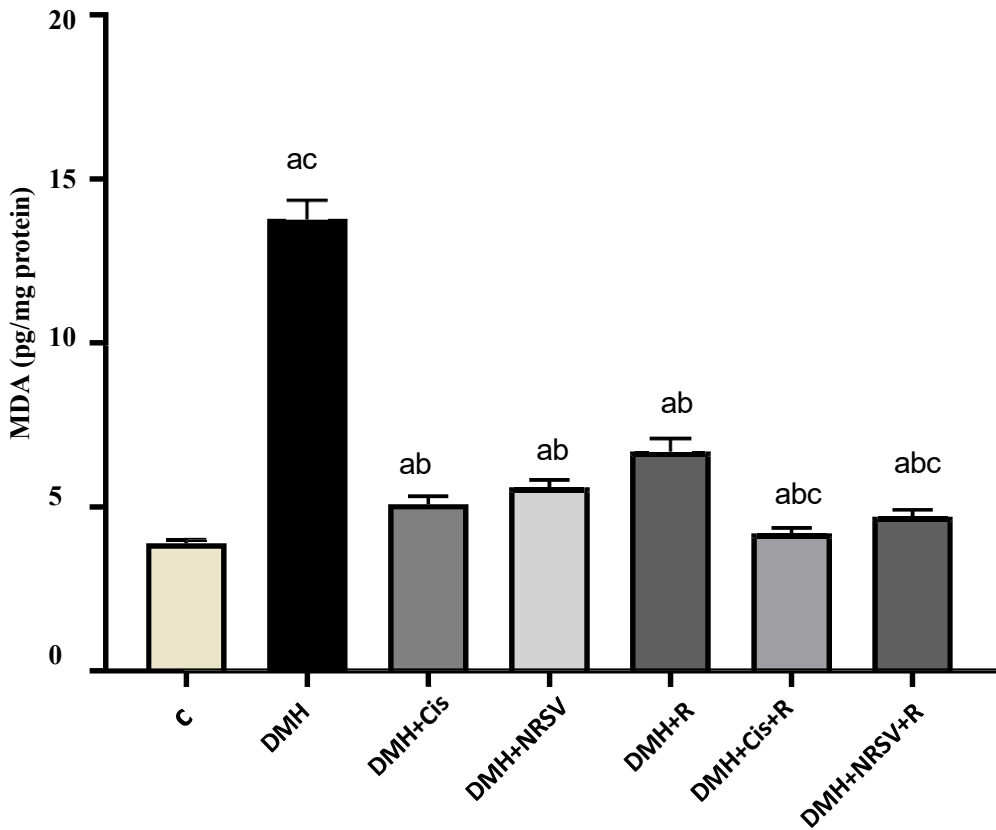
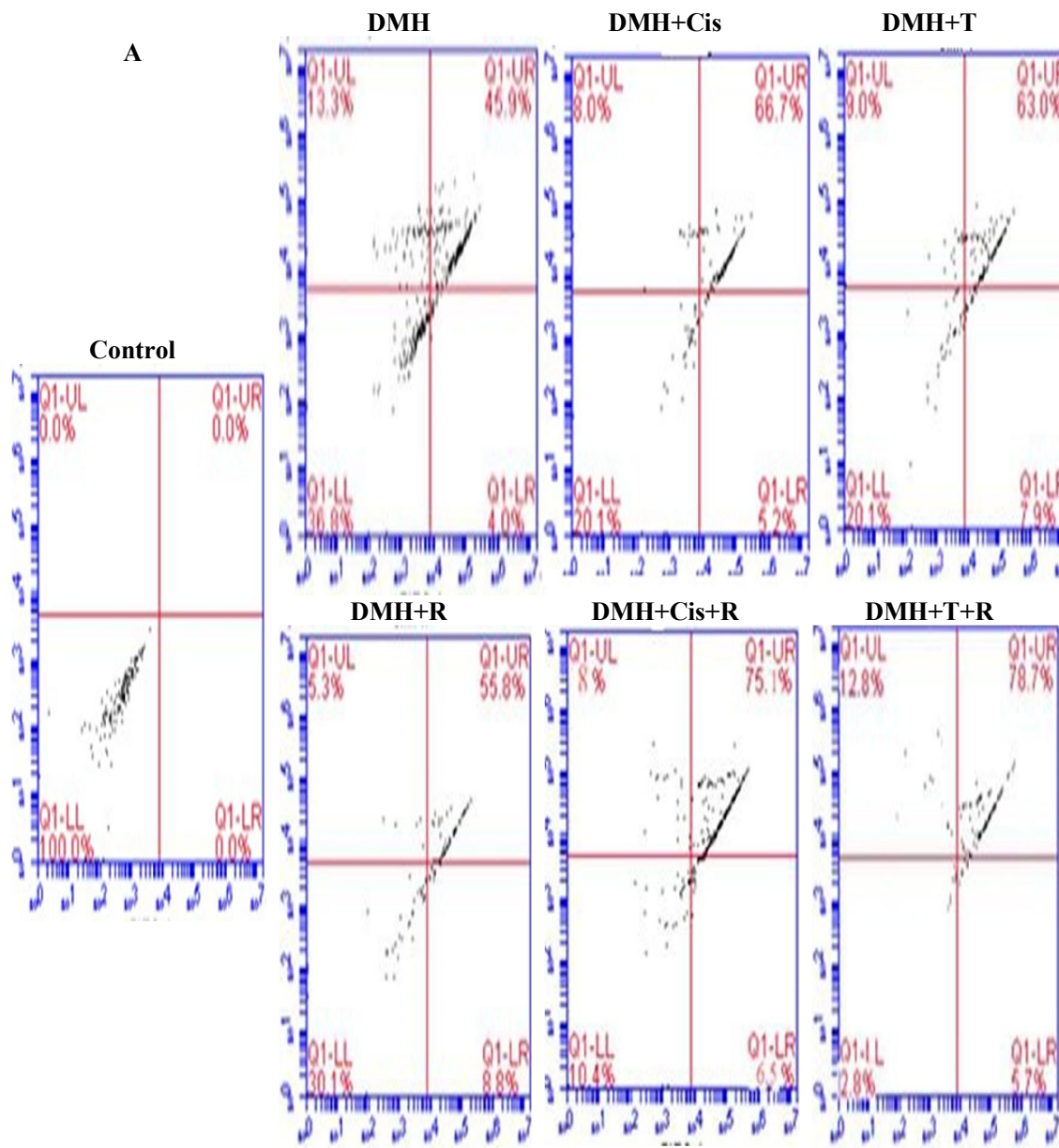


Fig. 3: Effect of treatment with nanoresveratrole on MDA levels

3.4. Evaluation of apoptosis by flow cytometry

As can be seen from Figure (4), apoptosis in the DMH group was significantly decreased compared to all other groups. Figure (4A) shows the results of one representative from each group, while Figure (4B) shows the results of means of three samples from each group. The early apoptotic cells% increased from 4% in the DMH group to 8.8, 7.9, and 5.2% in the DMH groups treated with radiation, NRSV, or cisplatin, respectively. Concomitant treatment with cisplatin+radiation elevated that percentage to 6.5%. The late apoptotic cells% increased from 45.9% in the DMH group to 55.8, 63.0, and 66.7% upon treatment with radiation, NRSV, or cisplatin, respectively. Concomitant treatment with NRSV+radiation or cisplatin+radiation elevated the late apoptotic cells percentage to 78.7 and 75.1%, respectively as shown in Figure (9A). It is noteworthy that the highest percentage of late apoptotic cells and the lowest percentage of viable cells were all reported in the group treated with NRSV+radiation



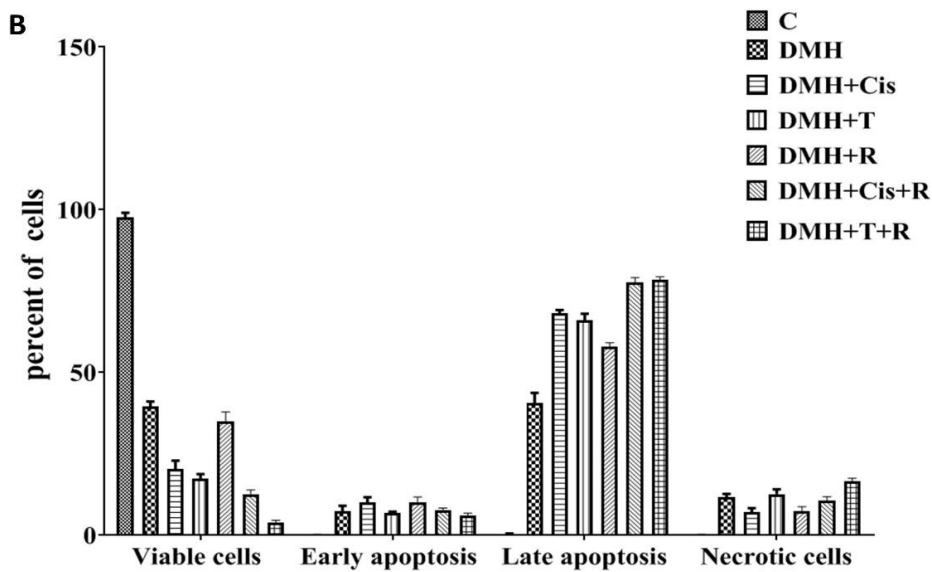


Fig. 4: Apoptosis detected by flow cytometry with Annexin V-FITC conjugated with PI staining. A. a representative from each group, B. the means of three samples from each group. C: control, DMH: dimethyl hydrazine, Cis: cisplatin, NRSV, R: radiation. Values are the mean \pm SEM (n=3). ^aSignificant change compared to the control group. ^bSignificant change compared to DMH group. ^cSignificant change compared to DMH+Cis. ^dSignificant change compared to DMH+T. The upper right and upper left quadrants represent the late apoptotic and necrotic cells, respectively. The lower left and lower right quadrants represent the viable and early apoptotic cells, respectively in percent of the total gated cells.

3.5. Histopathological findings

The colon of control rat revealed normal histological architecture of intestinal mucosa. The villi lined by a single layer of tall columnar cells with oval basal nuclei and numerous goblet cells dispersed between the columnar cells. The intestinal crypts were regularly arranged and lined by columnar cells. The intestinal glands appeared intact and lined by high cuboidal epithelial cells without any pathological alterations. Inflammatory reaction and hemorrhage were not detected (Figure A). On the other side, mice treated with DMH showed dysplastic changes, aberrant crypt foci (ACF) and intestinal glands with elongated nuclei, loss of cell polarity, increased mitotic activity, absence of goblet cells, and narrow lumens in epithelial cells of aberrant crypt foci. Cell dysplasia with various degrees were seen, with more packed glands that were uneven in shape and size. Complex glands with some areas of solid growth were detected (grade 4). Inflammatory cells, mainly lymphocytes and macrophages, infiltrating more than 20 per medium power field were noticed in lamina propria of the mucosa, muscularis mucosa, and submucosa score 3 (Figure 5B and C). Colon specimens from tumor bearing-mice treated with NRSV or exposed to γ -radiation showed significant mild and moderate dysplasia and anaplasia with irregular shape and size with some complexity of glands which contained apparent secondary structure (grade 2). Few goblet cells were detected with decreased number of inflammatory cells (10–20) per medium power field score 2 (Figure 5D and E, respectively).

Animals treated with cisplatin showed significant changes from untreated group (DMH). The intestinal glands and ACF showed loss of goblet cells, dysplasia of epithelial lining with pleomorphic nuclei, and reduction of mitotic activity. Some complexity glands contained apparent secondary structure (grade 2). More than 20 inflammatory cells permeated the mucosa's lamina propria, muscularis mucosa, and submucosa (score 3) (Figure 5F).

In the group treated with DMH+T+R, mucosal glands showed mild hyperplasia, mild degree of dysplastic changes and well differentiated intestinal glands (grade 1).

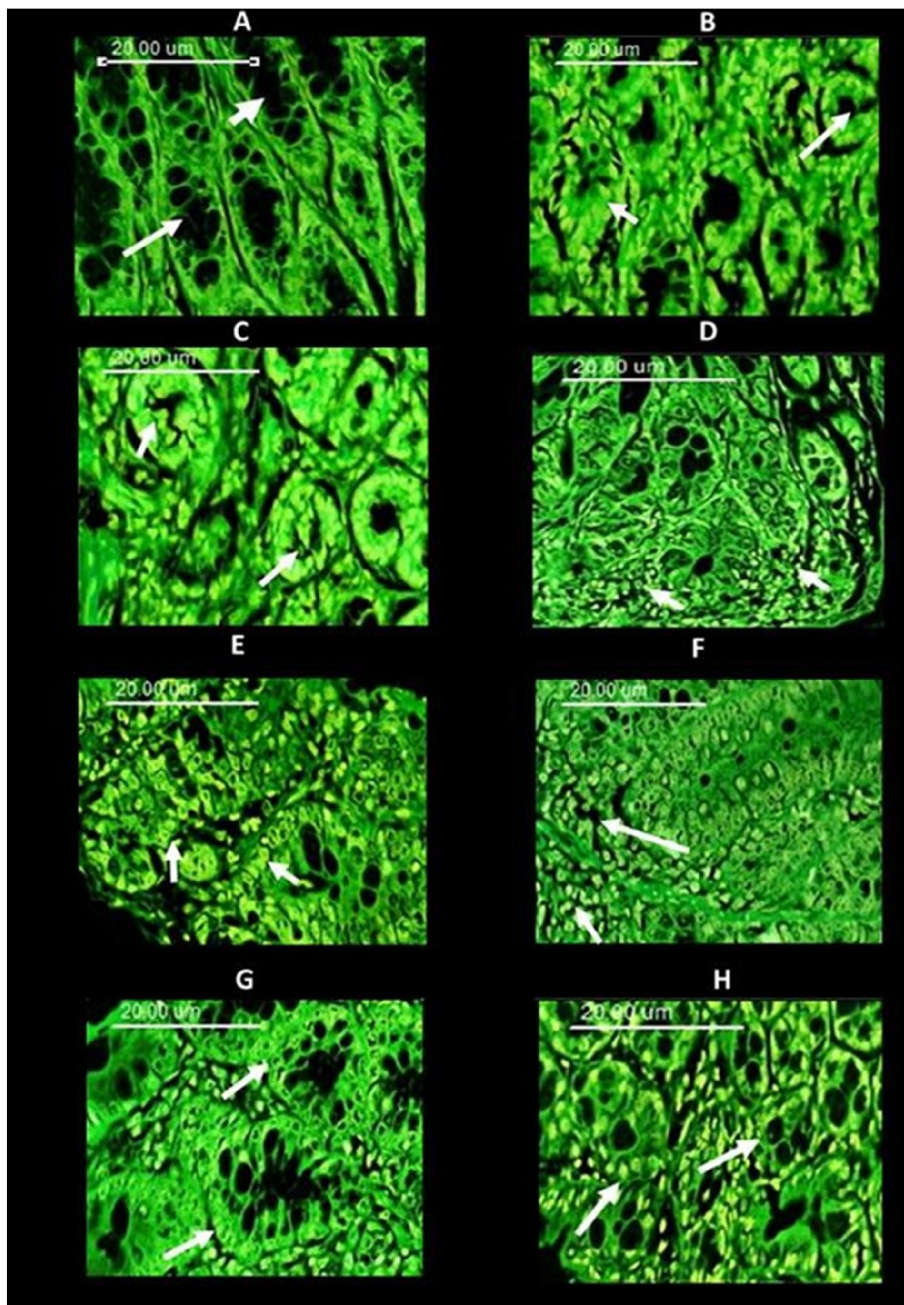


Fig. 5: Photomicrographs of rat colon sections stained with hematoxylin and eosin showing (A) Normal control, the arrow refers to intestinal glands lined by high cuboidal epithelial cells with numerous numbers of goblet cells, (B and C) Dysplasia of the mucosal lining epithelium as well as glandular structure with loss of goblet cells formation, pleomorphism in the cells as well as hyperchromatic nuclei of DMH treated animals. The arrow in (B) indicates crowded glands with irregularity in shape and size, and in (C) indicates intestinal glands with elongated nuclei, loss of cell polarity, increased mitotic activity and lack of goblet cells (D)

Dysplasia in lining glandular mucosal epithelium with goblet cells formation in the NRSV derivative treated group. The arrow refers to few numbers of goblet cells with decreased number of inflammatory cells (E) Dysplasia of the mucosal lining epithelium with pleomorphic nuclei (arrow) with goblet cells formation in the γ -irradiated group. (F) Massive inflammatory cells permeation in the lamina propria of the mucosa, muscularis mucosa and submucosa (arrow) in colon from cisplatin treated group. (G) Mild degree of dysplastic changes and well differentiated intestinal glands (arrow) in DMH+T+R group. (H) Moderate degree glandular epithelia dysplasia and more crowded glands (arrow) in DMH+cis+R group. (H&E x200).

Mild changes of absorptive and goblet cells. The lamina propria of the mucosa, muscularis mucosa, and submucosa was infiltrated with few inflammatory cells (less than 10, score 1) (Figure 5G).

Colon sections from the group treated with DMH+cis+R showed moderate changes of absorptive and goblet cells with moderate degree glandular epithelial dysplasia with more crowded glands and some complexity with glands containing apparent secondary structure grade 2. The lamina propria of the mucosa, muscularis mucosa, and submucosa was infiltrated with very few (less than 10, score 1) inflammatory cells (Figure 5H).

4. Discussion

The present study demonstrates that nano-resveratrole (NRSV) exerts significant anti-lymphangiogenic activity in a DMH-induced colon carcinogenesis model in male albino rats. NRSV attenuated oxidative stress, restored antioxidant defenses, modulated apoptotic responses, and improved histopathological outcomes. When combined with low-dose gamma irradiation, NRSV produced additive or potentially synergistic effect on suppressing lymphangiogenic signaling and reducing tumor burden. Collectively, these findings support the potential of NRSV as a chemopreventive or adjunct therapeutic agent in colorectal carcinogenesis, particularly through targeting the lymphatic metastatic niche.

Lymphangiogenesis is increasingly recognized as a critical facilitator of colorectal cancer metastasis. Pro-lymphangiogenic factors such as VEGF-C/VEGFR-3 signaling and LYVE-1-positive lymphatic endothelium correlate with nodal metastasis and poorer prognosis in CRC (Zheng *et al.*, 2014). The disruption of this axis has been shown to reduce lymphatic dissemination and metastatic colonization in preclinical models. In our study, NRSV-treated groups exhibited downregulation of lymphangiogenic markers (where measured) and histological features consistent with reduced lymphatic invasion, aligning with the concept that anti-lymphangiogenic strategies can complement cytotoxic approaches to curb metastasis (ElBakary *et al.*, 2022).

DMH-induced colon carcinogenesis is associated with oxidative DNA damage, lipid peroxidation, and depletion of antioxidant systems, creating a permissive environment for mutagenesis and clonal expansion (Kachur *et al.*, 2021). Elevated MDA and ROS with decreased GSH and TAC have been repeatedly reported in DMH models and are associated with tumor initiation and progression. In the current work, NRSV reduced lipid peroxidation and ROS while restoring GSH and TAC, supporting a rebalanced redox state that may hinder DNA damage accumulation and promote cellular protection. These redox-modulatory effect may also influence the tumor microenvironment, including immune cell function and stromal interactions, potentially impacting lymphangiogenic signaling indirectly (Yilgor and Demir, 2024).

Resveratrole (RSV) is known to exert anti-proliferative, pro-apoptotic, anti- inflammatory, and anti-angiogenic effect in various cancer models, with modulation of pathways such as JAK/STAT, PI3K/Akt, and VEGF signaling (Chen *et al.*, 2017). Nanoparticle encapsulation enhances RSV bioavailability, cellular uptake, and tumor targeting, which may amplify its therapeutic effect while reducing systemic toxicity (Öztürk *et al.*, 2024). In the present study, NRSV likely achieved superior intratumoral concentrations, enabling more effective suppression of lymphangiogenic processes and oxidative stress than free RSV. If available, co-localization studies or pharmacokinetic data would further support this premise.

Apoptosis remains a key mechanism by which anti-cancer agents suppress tumor growth. Annexin V flow cytometry revealed shifts in apoptotic populations across treatment groups, with NRSV-containing regimens showing modulation of early and late apoptosis. The relationship between apoptosis and lymphangiogenesis is nuanced: apoptotic tumor cells can release factors that influence the tumor vasculature and immune milieu. Our data suggest that NRSV can tilt the balance toward tumor cell clearance while dampening pro-lymphangiogenic signaling, potentially reducing the risk of viable metastatic seeds in draining lymphatics (Hagan *et al.*, 2025).

4.1. Radiation Interactions and Microenvironment Modulation

Low-dose gamma irradiation can alter tumor vasculature and lymphatic remodeling in dose- and schedule-dependent ways. In some contexts, irradiation may normalize tumor perfusion and improve drug delivery, while in others it may transiently upregulate pro-angiogenic/lymphangiogenic pathways or induce inflammatory responses that promote metastasis. In our study, radiation combined with NRSV

yielded enhanced anti-tumor effect, suggesting a potential synergistic interaction. Mechanistically, radiation-induced ROS and DNA damage could sensitize tumor cells to NRSV-mediated pro-apoptotic signaling, while anti-lymphangiogenic effect may hinder radiation-driven lymphatic dissemination (El Bakary *et al.*, 2020). Further mechanistic dissection is required to delineate the balance of these interactions.

The histopathology findings corroborate the biochemical and flow cytometric data. Groups showed preserved mucosal architecture with minimal dysplasia, whereas DMH alone induced dysplastic changes progressing toward adenocarcinoma in susceptible animals. NRSV-treated groups displayed reduced dysplasia, lower incidence and multiplicity of adenomas/adenocarcinomas, and diminished invasion. Immunohistochemical analyses aligned with the histology, showing reduced lymphatic density in NRSV groups, which supports the histopathological evidence of anti-lymphangiogenic activity. These observations are consistent with the proposed mechanism whereby NRSV impedes the formation or remodeling of lymphatic vessels within or around neoplastic lesions (Medhat *et al.*, 2017). Our findings echo prior reports demonstrating anti-angiogenic properties of RSV and its derivatives in various tumor models, with nanoparticle formulations enhancing efficacy. Previous studies have shown CRC models showing reduced tumor growth and microvessel density upon RSV treatment, with modulation of VEGF pathway signaling (Rajasekar *et al.*, 2019). However, data specifically addressing NRSV-mediated anti-lymphangiogenesis in DMH-induced colon cancer are scarce, making our study a novel contribution to the field. Differences in study design, dosage, and delivery system should be considered when comparing across studies (Wang *et al.*, 2024).

4.2. Strengths, Limitations, and Future Directions

4.2.1. Strengths:

A multi-arm design enables dissection of DMH-induced carcinogenesis, NRSV efficacy, and the impact of radiation on lymphangiogenic and oxidative stress parameters. The integration of biochemical, apoptotic, and histopathological endpoints provides a holistic view of treatment effect.

4.2.2. Limitations:

The study may be limited by sample size per group for certain endpoints, potential variability in DMH-induced tumor burden, and the absence of long-term survival data. If not performed, inclusion of lymphangiogenic molecular markers (VEGF-C/D, VEGFR-3, LYVE-1) would strengthen mechanistic conclusions. Additional limitations may include the translatability of a rodent model to human CRC and the generalizability of radiation scheduling to clinical practice.

4.2.3. Future directions:

Validate these findings with larger cohorts and extended time points, perform mechanistic studies on lymphangiogenic signaling cascades, evaluate pharmacokinetics of NRSV, and explore combination regimens with other standard-of-care agents. Investigate immunomodulatory effect, given that lymphatic remodeling intersects RSV with anti-tumor immunity. If feasible, assess survival outcomes and metastatic burden beyond the colon to provide a more comprehensive translational perspective.

4.2.4. Clinical and Translational Implications

By targeting the lymphatic dissemination route, NRSV may complement conventional cytotoxic therapies and radiotherapy to reduce metastatic spread in CRC. The redox-modulating properties of NRSV also suggest potential synergy with immunotherapies, as oxidative stress can influence antigen presentation and immune cell function. While promising, clinical translation will require careful dose optimization, robust toxicity profiling, and demonstration of efficacy in models that more closely mimic human disease (e.g., patient-derived xenografts or genetically engineered mouse models).

5. Conclusions

Nano-resveratrol demonstrates strong potential as an anti-lymphangiogenic agent in DMH-induced colon carcinogenesis, acting through a combination of oxidative stress attenuation, restoration of antioxidant defenses, and regulation of apoptotic pathways. The observed histopathological improvements and reduced lymphatic involvement support further development of NRSV, including optimization of dosing, scheduling, and exploration of additive or synergistic effect with radiotherapy.

Future work should focus on validating molecular targets within the lymphangiogenic axis and translating these findings toward clinically relevant CRC prevention or treatment strategies

Declarations

Ethics approval and consent to participate

All experiments were performed in accordance with ARRIVE guidelines. The study was approved by the Ethical Committee (REC) of the NCRRT, Atomic Energy Authority, Cairo, Egypt.

Consent for publication

Not Applicable

Availability of data and material

All data presented in this manuscript are reported in the manuscript.

Competing interests

The authors declare no competing interests.

Authors' contributions

M.H.O. designed the study. N.M.E. and M.H.O. carried out the practical work. E.K. performed the data analysis and wrote the draft of the manuscript. S.M.E. synthesized and characterized nanoresveratrole. S.M.E. , E.Kcritically read and revised the manuscript. All authors approved the manuscript.

References

Chen, Z., R. Zhu, J. Zheng, C. Chen, C. Huang, J. Ma, ... & J. Zheng, 2017. Resveratrole inhibits proliferation yet induces apoptosis by suppressing STAT3 signals in renal cell carcinoma. *Oncotarget*, 8(30), 50023.

Deng, R., G. F. Zong, X. Wang, B. J. Yue, P. Cheng, , T R. Zao ... & Y. Lu, 2024. Promises of natural produRSV as clinical applications for cancer. *Biochimica et Biophysica Acta (BBA)-Reviews on Cancer*, 189241.

ElBakary, N. M., A. Z. Alsharkawy, Z.A. Shouaib and E.M. Barakat, 2020. Role of bee venom and melittin on restraining angiogenesis and metastasis in γ -irradiated solid ehrlich carcinoma-bearing mice. *Integrative Cancer Therapies*, 19, 1534735420944476.

ElBakary, N.M., S.A. Hagag, M.A. Ismail and W.M. El-Sayed, 2022. New thiophene derivative augments the antitumor activity of γ -irradiation against colorectal cancer in mice via anti-inflammatory and pro-apoptotic pathways. *Discover Oncology*, 13(1), 119.

Gao, L., and A. Zhang, 2023. Low-dose radiotherapy effect the progression of anti-tumor response. *Translational Oncology*, 35, 101710.

Hagan, C.E., V.M. Sheehan, C.M. Rezanka, et al., 2025. Apoptotic cells promote circulating tumor cell survival and metastasis. *Commun Biol* 8, 1121 .<https://doi.org/10.1038/s42003-025-08541-7>

Kachur, O., L. Fira, P. Lykhatskyi, D.Fira, and I. Stechyshyn, 2021. The state of pro-and antioxidant systems in rats with DMH-induced colon carcinogenesis on the background of extracorporeal detoxification. *Pharmacia* (0428-0296), 68(4).

Li, B., O.Q.B. Allela, W.H. Alkhazali, et al., 2025. Resveratrol in oral cancer: a systematic review of preclinical studies on its anticancer mechanisms and therapeutic potential. *Med. Oncol.*, 42, 329. <https://doi.org/10.1007/s12032-025-02903-1>

Liu, X., Y. Gao, F. Yang, M. Qian, S. You, X. Wang, F. Qin, M. Xiang and W. Guo, 2025. A Review of Resveratrole and its Nanoformulation in Cancer Therapy. *Anticancer Agents Med Chem.* 25(16):1188-1197. doi: 10.2174/0118715206372305250319064431. PMID: 40176695.

Medhat, A.M., K.S. Azab, M. M. Said, N. M. El Fatih and N. M. El Bakary, 2017. Antitumor and radiosensitizing synergistic effect of apigenin and resveratrole against solid Ehrlich carcinoma in female mice. *Tumor Biology*, 39(10), 1010428317728480.

Öztürk, K., M. Kaplan and S. Çalış, 2024. Effect of nanoparticle size, shape, and zeta potential on drug delivery. *International journal of pharmaceutics*, 666, 124799.

Rajasekar, J., M. K. Perumal and B. Vallikannan, 2019. A critical review on anti-angiogenic property of phytochemicals. *The Journal of Nutritional Biochemistry*, 71, 1-15.

Wang, C., J. Xu, X. Cheng, et al., 2024. Anti-lymphangiogenesis for boosting drug accumulation in tumors. *Sig Transduct Target Ther* 9, 89. <https://doi.org/10.1038/s41392-024-01794-4>

Wu, Y.H., Y.R. Wu, B. Li and Z.Y. Yan, 2020. Resveratrole: A review of its pharmacology activities and molecular mechanisms. *Fitoterapia*. 2020 Sep;145:104633. doi: 10.1016/j.fitote.2020.104633.

Yilgor, A. and C. Demir, 2024. Determination of oxidative stress level and some antioxidant activities in refractory epilepsy patients. *Sci Rep* 14, 6688. <https://doi.org/10.1038/s41598-024-57224-6>

Zhang, J. Y., H. Li, M.J. Zhang and Z.J. Sun, 2025. Lymphangiogenesis orchestrating tumor microenvironment: Face changing in immunotherapy. *Biochimica et Biophysica Acta (BBA)-Reviews on Cancer*, 189278.

Zheng, W., A. Aspelund and K. Alitalo, 2014. Lymphangiogenic factors, mechanisms, and applications. *The Journal of Clinical Investigation*, 124(3), 878-887.

Zhou, J., Q. Yang, S. Zhao, L. Sun, R. Li, J. Wang and D. Wang, 2025. Evolving landscape of colorectal cancer: global and regional burden, risk factor dynamics, and future scenarios (the Global Burden of Disease 1990-2050). *Ageing Research Reviews*, 102666.